

Design optimization of a silicon/organic hybrid micro-resonator for 2D WH/TS optical encoding

K. S. RESMI*, PRITA NAIR

Department of Physics, SSN College of Engineering, Kalavakkam, India 603 110

Optimum design for the realization of a novel dynamic WH/TS optical encoder by fast EO tuning of defect mode of an EO polymer infiltrated 1D Si Photonic Crystal resonator has been presented. Uniformity in transfer characteristics, line width, efficiency, size, and power usage are the metrics used for optimization. In the design, chip duration, wavelength selection and time gating functions can be programmed to provide adaptive OCDMA encoding providing easy low power, low cost upgrade in capacity of standard 10Gbps systems in access networks to about 200Gbps. Availability of wide bandwidth and reconfigurable codes accounts for the improved number of users ensured by the single reconfigurable device design.

(Received September 12, 2016; accepted June 7, 2017)

Keywords: Optical code division multiple access (OCDMA), Photonic crystal(PhC), Electro-optic(EO) effect

1. Introduction

Incoherent optical code division multiple access (OCDMA) is a technology that fulfils, the demands of expanding internet utilities, such as security, cost and power efficiency and enhanced bandwidth. It is a multiple access technology where in the data of each user or group of users utilizing the same network resources are differentiated on the basis of unique code words assigned to each of them. This code word is transmitted during the ON period of the user data. In 1D OCDMA, the ON period is thus divided into smaller time chips and code represents the ON-OFF sequence of these time chips. The number of users that can be accommodated on the same network resource depends on the length of the code word or the number of time chips. But increasing time chips is not a viable solution. Therefore 2D wavelength hopping time spreading (WH/TS) OCDMA scheme where an extra dimension in terms of wavelength used in each time chip, has emerged as the possible solution. This increases the number of users without increasing the time chips. Hence to come up with a low cost solution for encoding and decoding suitable for implementation in access networks becomes essential.

In the optical encoders reported in literature [1-3], the output of incoherent broadband source is modulated using the time encoded user data and then filtered using either series of FBG's, SSFBG's, or with AWG with the time delays between the successive wavelength pulses suitably adjusted. But in all these, the hardware implementation is specific for a particular code and has only limited tunability once physically implemented. The need of the hour, with required bandwidths slated to touch hexa bytes, is a single low cost device which can be dynamically programmed to implement any code as and when required. This would enable dynamic software controlled secure coding and decoding. This paper presents the design of a

device based on fast, low power EO tuning of the resonant frequency of a silicon micro-resonator realized as a defect in EO polymer infiltrated 1D Silicon photonic crystal (PhC) waveguide. The design implementation is achieved by combining strong optical confinement abilities of silicon and good EO modulation efficiency of polymer. The design presented here is a generic one suitable for use with any EO polymer of refractive index lower than that of Si. Therefore in this study readily available polymer polystyrene has been used for theoretical and practical modelling of the design. EO coefficient is assumed as 80 pm/V for modelling purpose, achievable when doped with proper chromophore and poled appropriately.

For 2D WH/TS encoding, the device should perform wavelength selection (to represent high bit of code sequence in time domain) with a time delay (representing low bits of code sequence) and should provide adequate time gating (to maintain the selected wavelength for a chip duration). The silicon-organic hybrid design is so implemented that it does wavelength selection within the incoherent optical source bandwidth (C-band of electromagnetic spectrum), for voltages above 0 Volts. At zero bias wavelength selection happens outside the C-band, resulting in nil transmission and hence provides the appropriate time delay. Duration of voltage applied for wavelength selection decides the chip rate.

The forthcoming section explains the operating principle and working of the design. This is followed by results of the preparation of the polymer sample and experimental verification of the complex dielectric constant using spectroscopic ellipsometry. The transmission characteristics of different device configurations have been modelled using finite element modelling (FEM) incorporating the experimentally observed dispersion characteristics of the polymer in the 1500nm-1600nm band.

2. Basic theory of operation

According to Yablonovitch [4] and John [5], the photonic modes of the material are influenced by structures with periodic variation in refractive index. The localized photonic states results due to defect in periodicity [6]. A point defect in a periodic PhC structure, gives rise to defect modes in the transmission spectrum.

Silicon-based electro-optic effect requires P and N doping on either side of the silicon waveguide and power consuming carrier injection across the waveguide as Si is not an electro-optic material. The EO polymer is a material with high pockel's coefficient and low half-wave voltage thereby providing a low power alternative to realize electro-optic control of output power. This EO polymer can be infiltrated into a waveguide suitably modified in to a resonator form [7]. If a broadband light source is incident on this structure, the transmitted wavelength can be electro-optically tuned.

A Si waveguide with dimensions in the order of few hundreds of nanometres with air on all 3 sides and oxide layer in the bottom can be easily realized on SOI wafers, and will ensure polarized single mode operation in the C band. A periodic 1-D photonic crystal, etched into this, with appropriate lattice constant gives rise to band gap in the desired wavelength range while a defect introduced into the perfectly periodic structure, allows transmission at a defect mode within the original band. The band gap and defect mode depends on the periodicity and dimensions of periodic holes (low index regions) in the silicon slab. A set of periodically spaced three holes on Si waveguide on either side of a central Si region acts as Bragg mirrors on either sides of a Si cavity, giving a Fabry-Perot effect (Refer to figure 1).

When doped polystyrene of RI 1.59 is infiltrated in to quarter wavelength sized holes, this defect mode occurs at 1570nm, as shown in Fig. 2, which can be tuned by voltage induced index variation.

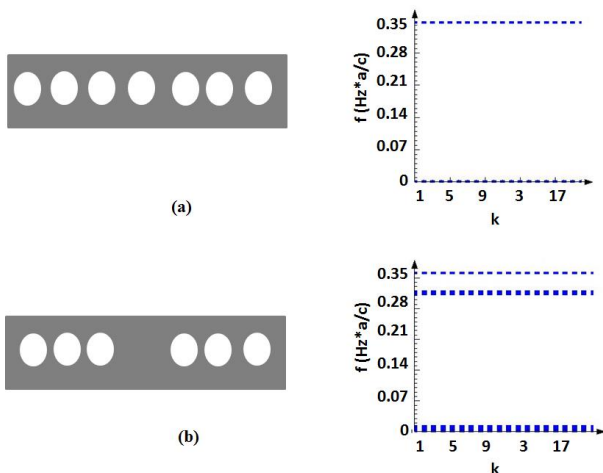


Fig. 1. The (a) band gap of a perfectly periodic air filled PhC in Si and (b) defect mode of air filled PhC with point defect.

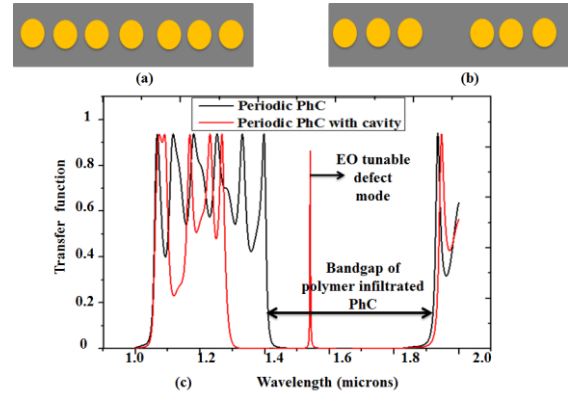


Fig. 2. The (a) Polymer infiltrated periodic PhC and (b) polymer infiltrated PhC with defect in periodicity (c) comparison of transfer their characteristics

The refractive index change of the EO polymer, due to voltage change is governed by [8]:

$$\Delta n_{poly} = \frac{-n_{poly}^3 \gamma_{33} f^3 U}{2d} \quad (1)$$

Where, n_{poly} is the refractive index of polystyrene, U is the applied voltage, γ_{33} , the electro-optic coefficient of the doped polymer assumed to be 80pm/V, d is the distance between the electrodes and f is the local field factor calculated as :

$$f = \sqrt{\frac{V_g^{BULK}}{V_g^{PC}}} \quad (2)$$

In equation (2), V_g^{BULK} is the group velocity of bulk polystyrene and V_g^{PC} is that of the photonic crystal, given by $V_g^{PC} = \frac{C}{69}$, resulting in f as 6.6 [9].

The variation of refractive index of silicon with wavelength is given by Sellmeier's equation[10]:

$$n(\lambda)^2 = 11.6858 + \frac{0.939816}{\lambda^2} + \frac{0.00810461 \lambda_1^2}{\lambda^2 - \lambda_1^2} \quad (3)$$

where λ is the wavelength in μm and reference wavelength $\lambda_1 = 1.1071 \mu\text{m}$.

3. Design and working of the basic resonator

The design consists of a micro beam silicon waveguide with dimensions of $8 \mu\text{m} \times 240 \text{nm} \times 250 \text{nm}$ realizable on a SOI wafer. The PhC structure with holes of diameter 215nm each and lattice period of 400nm with a defect at the centre is illustrated in the schematic given in figure 3. The EO polymer (doped polystyrene) is

infiltrated into the holes. Distance of separation between the electrodes is kept as 325nm so that wave guiding is not disturbed.

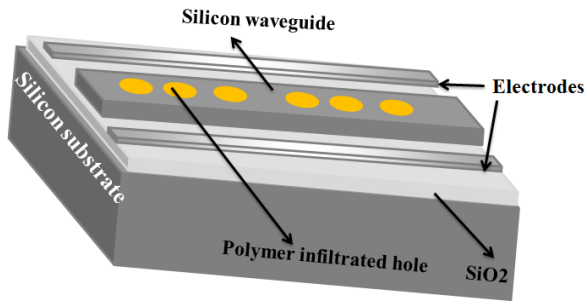


Fig. 3. Schematic of the EO resonator

Signal from a broadband optical source (C-band), undergoes multiple reflection within the cavity and the electro-optic polymer allows transmission of the resonant wavelengths (defect modes), depending on applied voltage. In order to build a realistic model of the device performance, dispersion characteristics of the polymer in the region of interest also needs to be modelled. For this, a thin film sample of the polystyrene was prepared and spectroscopic ellipsometric studies were conducted in the 1500-1600 nm region. These values have been used for the theoretical simulation.

4. Experimental determination of dispersion characteristic of polystyrene

0.2mg of polystyrene (Molecular weight ~ 280,000g/mol) purchased from Sigma –Aldrich, was dissolved in 20 ml of Toluene (anhydrous, 99.8%) using a magnetic stirrer with hot plate maintained at 60°C. A thin film was spun onto a RCA cleaned 20µm thick silicon wafer using a programmable spin coater (Apex Equipments/spin NXG-P1). The spin was carried out at 500 r.p.m for first 10 seconds, for uniform spread and then increased to 3000 r.p.m for 50 seconds. The resulting 1 µm thick thin film sample was then analyzed using Woollam spectroscopic ellipsometer.

The experimentally observed variation in refractive index of polystyrene with wavelength from the ellipsometric analysis can be represented by the equation [11]:

$$n_{poly}(\lambda) = -(3.21 \times 10^{-5} \lambda) + 2.08 \quad (4)$$

Where $n_{poly}(\lambda)$ is the refractive index of polystyrene at wavelength λ .

5. Application of the EO tuned resonator as 2D optical encoder

Consider a 10 Gbps bit stream (OC-192) using NRZ scheme with a time period of 100ps, chipped in- to four 25ps time slots. Consider a 2D coding scheme in OCDMA using 2 wavelengths. For this 4-bit TS scheme, there are 2 distinct possibilities to implement 2D wavelength scheme, avoiding all its cyclic variations to reduce complexity. One is a code with the 2 high bits occurring with a 25ps gap, and second is a code with 2 high bits occurring with a higher or lower gap say for example 1010 and 1100 respectively. Using a 2 wavelength scheme, each of these can be implemented in 3 different ways. Let us say that the 2 wavelengths selected are indicated as B and Y. Then 1100 can form 3 distinct code implementations as BB00, YY00 and BY00 as illustrated in figure 4. Even if all other combinations have been left out so that simple filter bank based the decoding scheme can be thought of, this would mean 6 codes for a 4bit 2D WH/TS encoding per pair of wavelengths. 6 codes imply a 6X increase in transmission rate to 60Gbps bandwidth for a pair of wavelengths. Therefore if an incoherent source covering C band is employed, transmission bandwidth in access networks can be dynamically scaled using encoders which can be programmed to select different wavelength pairs within the source bandwidth. The voltage applied across the beam will determine the wavelength of the transmitted chip during high bits (1) and at 0V when no wavelength is transmitted (0 bit) represents the delay between the 2 high bits. Duration of this applied voltage maintains the time slot (25ps).

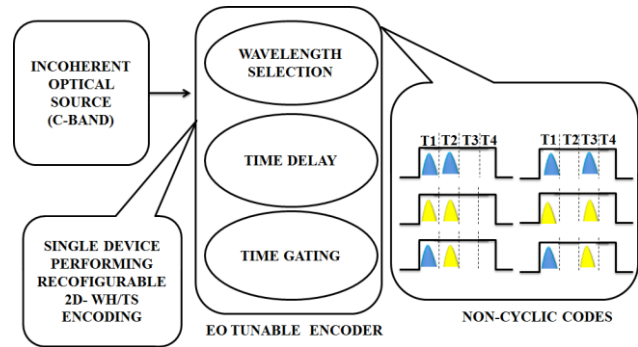


Fig. 4. Block diagram of the functioning of EO tunable micro resonator as encoder

6. FEM simulation of the device

6.1. Basic design: Design 1

This design gives a tuning sensitivity of 5.6 nm/V in C band (Refer to Fig. 7). Transmittance is found to be above 90% for each wavelength selected while line width of the curves are found to vary from 4.1 to 1.2 nanometers over the voltage range from 0 to 7 volts .

To reduce this non-uniformity in the output characteristics, alternate design is considered with hole shape changed from circular to rectangular.

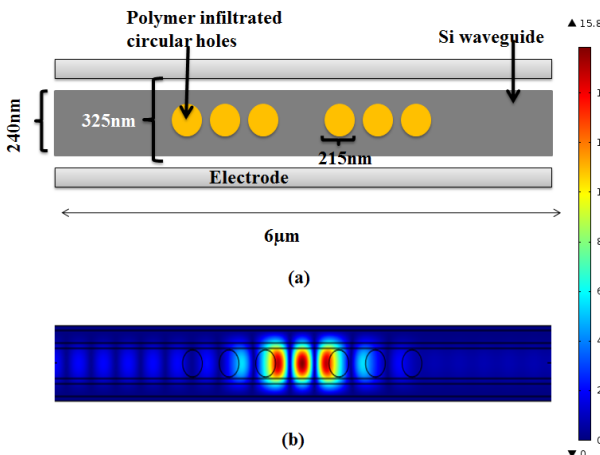


Fig. 5. The (a) schematic of the basic device design (b) Sample field distribution at resonance

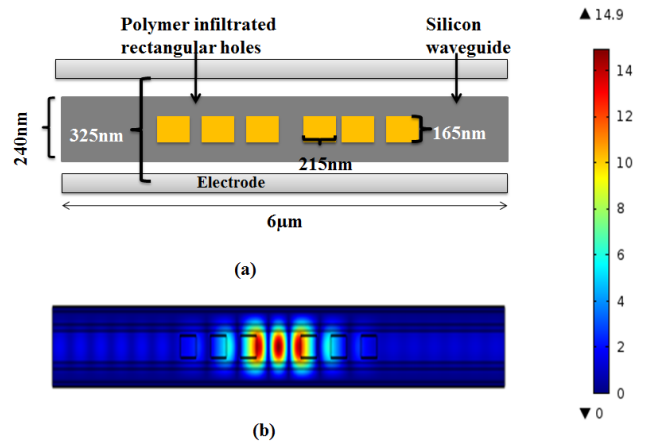


Fig. 6. The (a) Schematic of the design 2 (b) sample field distribution at resonance

Here, though line width of wavelength selection curve is higher than in the previous design, it is found that design 2 gives higher tuning sensitivity of 7.25 nm/V in C band as in figure 7. The transfer function of more than 0.9 remains uniform for the entire range of applied voltage. Thus, shifting to rectangular holes reduces the required applied voltage range to 5V for same wavelength range.

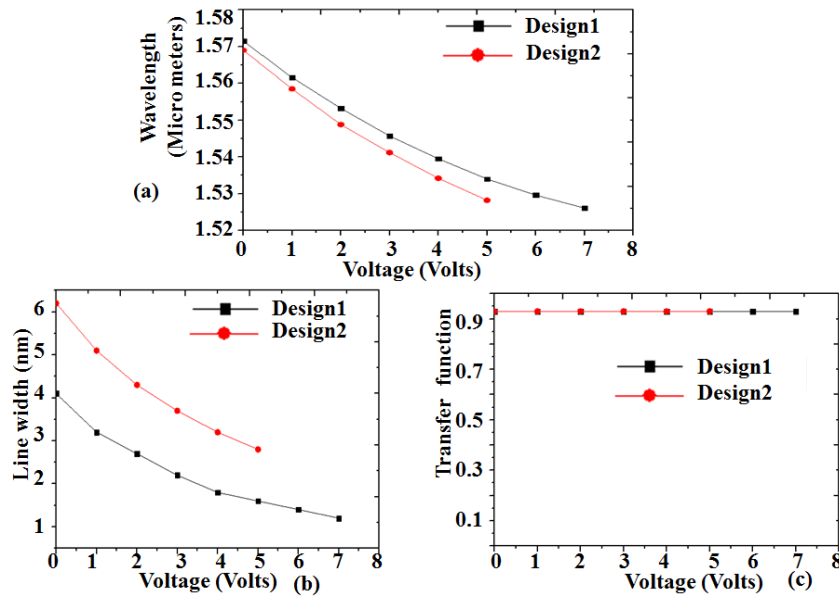


Fig. 7. Comparison of (a) Wavelength tuning, (b) line width and (c) transfer characteristics of design 1 and design 2

6.2. Design 3

The previous designs needs to be modified in order to reduce the line width further .In the above designs, the non-uniform line width indicates lack of finesse which implies a requirement of better reflectivity of the Bragg mirrors.

Therefore in addition to an extra pair of holes a rectangular hole of half wave optical length is also used on either sides of the cavity.

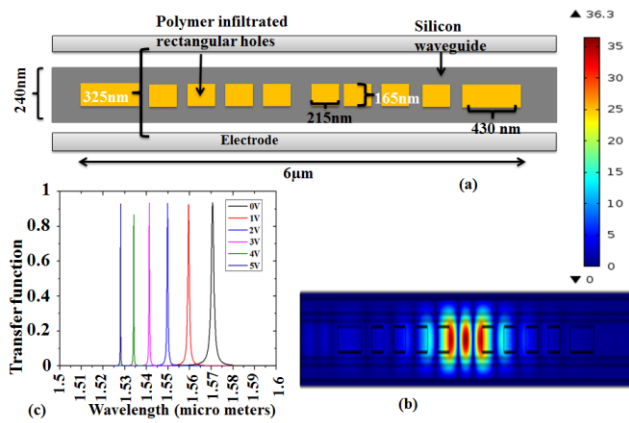


Fig. 8. The (a) Structural details of design 3 (b) sample field distribution at resonance (c) Voltage dependent tuning curve of design 3

This design modification is thus found to ensure more uniformity in the linewidth of the defect modes.

7. Result and discussion

The proposed encoder design is found to provide dynamic wavelength selection as well as time delay and time gating. Tuning curve of the design in Fig. 8(c) shows good transmittance (within 85-95%) and improved line width (from 0.8nm to 0.2 nm) within the C-band. The voltage requirement is found to be within 5 volts. Compact and less complex design adds to ease in practical implementation of the design. A comparison of performance of all the different designs is evaluated and is presented in Table 1.

Table 1. Comparative study of the simulation results of designs 1, 2 and 3

Voltage (Volts)	Design 1			Design 2			Design 3		
	WL (nm)	TF	LW (nm)	WL (nm)	TF	LW (nm)	WL (nm)	TF	LW (nm)
0	1571.5	0.93	4.1	1569	0.93	6.2	1570.5	0.93	1.5
1	1561.6	0.93	3.2	1558.5	0.93	5.1	1559.4	0.93	0.8
2	1553.2	0.93	2.7	1548.8	0.93	4.3	1549.7	0.93	0.5
3	1545.7	0.93	2.2	1541.2	0.93	3.7	1541.3	0.93	0.3
4	1539.5	0.93	1.8	1534.2	0.93	3.2	1534.1	0.86	0.3
5	1534	0.93	1.6	1528.2	0.93	2.8	1528	0.93	0.2
6	1529.6	0.93	1.4						
7	1526.1	0.93	1.2						

The virtual prototype of the structure of design 3 using CAD tool Intellisuite is shown in Fig. 9.

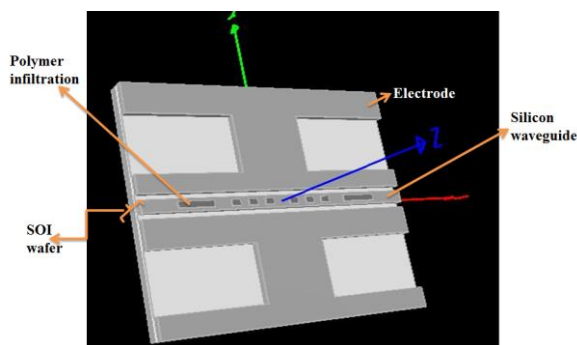


Fig. 9. Virtual prototypes of the device design 3 on SOI wafer using MEMS CAD tool

8. Conclusion

The working and design optimisation of a novel adaptive 2 D WH/TS OCDMA encoder based on fast EO tuning of polymer infiltrated Si waveguide is

demonstrated. The available wide spectral bandwidth of incoherent sources typically 35nm and re-configurability of codes as required without changing the device implemented and ensures dynamic adaptation to support more number of users or flexible line rates. The square shaped polymer infiltrated holes enhances tuning sensitivity compared to circular holes by 2 nm/V and the addition half wave hole provides improved line width. This design of the WH/TS encoder is capable of improving the transmission rate dynamically from 10 Gbps to about 200Gbps, at low operational expenses both optical and electrical.

Acknowledgments

The authors would like to thank Nanotechnology Research Center, SRM University, Chennai, for access to spin coating unit. The authors would also like to thank Microelectronics and MEMS Laboratory, IITM, Chennai, for spectroscopic ellipsometry testing and Dr. Satish Kumar, Chemical Engineering department, SSN Engineering college, Chennai for discussion sessions on polymer characterization.

References

- [1] Ye Zhang, Hongwei Chen, Zhijian Si, Heng Ji, Shizhong Xie, *IEEE Photonics Technology Letters* **20**, 891 (2008).
- [2] K. Kitayama, Xu Wang, Naoya Wada, *Journal of Lightwave Technology* **24**, 1654 (2006).
- [3] S. Yegnanarayanan, A. S. Bhushan, B. Jalali, *IEEE Photonics Technology Letters* **12**, 573 (2000).
- [4] Eli Yablonovitch, *Phys. Rev. Lett.* **58**, 2059 (1987).
- [5] S. John, *Phys. Rev. Lett.* **53**, 2169 (1984).
- [6] J. D. Joannopoulos, Pierre R. Villeneuve, Shanhui Fan, *Nature* **386**, 143 (1997).
- [7] T. Baehr-Jones, M. Hochberg, Guangxi Wang, R. Lawson, Y. Liao, P. A. Sullivan, L. Dalton, A. K.-Y. Jen, A. Scherer, *Opt. Express*. **13**, 5216 (2005).
- [8] Matthieu Roussey, Fadi I. Baida, Maria-Pilar Bernal, *J. Opt. Soc. Am. B.* **24**, 1416 (2007).
- [9] Lingyu Liu, Daquan Yang, Huiping Tian, Yuefeng Ji, *Optics Communications* **285**, 171 (2012).
- [10] E. D. Palik, Editor, *Handbook of Optical Constants of Solids*, San Diego, CA, Academic, (1998).
- [11] K. S. Resmi, Prita Nair, in 2015 Workshop on Recent Advances in Photonics (WRAP), p. 1-4, IEEE (2017).

*Corresponding author: resmiks@ssn.edu.in